

## **Appendix I: Details in Background Information on Soil Profile and Properties Issues**

INTENTIONALLY LEFT BLANK

## **Appendix I: Details in Background Information on Soil Profile and Properties Issues**

A major technical issue in the parametric analyses relates to the difficulties in defining the appropriate input parameters, especially regarding ground motion hazard levels and site soil properties to obtain meaningful and relevant cask response for review of cask design applications. Ultimately, in order for the library of cask response solutions to be usable to the Nuclear Regulatory Commission staff in the safety review of cask design licensing applications, there needs to be a relatively simple and systematic way for cross comparison of ground shaking input as well as soil properties between the parametric study and the site-specific applications.

It would be logical to separate ground motion from soil properties issues. The implication of site soil properties toward ground motion site response in the context of the parametric study would be quite different from conventional design projects, where site response analysis is primarily part of the seismic study for defining the hazard level of ground motion to meet design requirements. Since the inherent process involves calibrating ground surface shaking, a different treatment would be required to implement site soil properties to the specifics of parametric analyses. The adopted procedure has a built-in safeguard for achieving the properly targeted ground surface shaking, so long as a consistency in soil parameters (including modulus and damping) is maintained between deconvolution solution of input motion and the resultant coupled cask response models. Lam et al. [1] documented the detailed procedure to achieve the intended ground shaking input to the coupled cask/pad/foundation model. Furthermore, it is important to match appropriate soil properties with issues related to the coefficient of restitution, which would be dominated by the localized surface soil condition. This discussion provides further background information on the soil profiles summarized in Figure 3.5 in the main text.

An extensive literature search was conducted in the parametric study to gather information on generic site soil properties, particularly those used in the nuclear power industry. Eventually, the selected soil profiles and properties adopted for the parametric study were based on two Electric Power Research Institute (EPRI) reports [2 and 3]. For example, Figure I-1, which shows shear wave velocity profiles for generic nuclear power plant sites, has been extracted from the 1989 EPRI report [2]. The benchmark soil profiles in the parametric study (referred to as stiff soil site conditions) are based on the Standard Profile in Figure I-1. Similarly, the Lower Range Profile in this figure was used to generate the soft soil profile. After discretization, the two referenced (referred to as Standard and Lower Range) shear wave velocity profiles led to the two low-strain shear wave velocity (referred to as stiff and soft soil) profiles in the site response models as shown in Figure I-2.

Deconvolution analyses were performed to provide soil column base motions at 140-ft depth for the two cited stiff and soft soil profiles as well as the upper bound rock profiles using the SHAKE91 program [4]. In these analyses, the parametric study adopted the 1993 EPRI procedure [3] on depth-dependent sand modulus and damping ratio versus shear strain curves as shown in Figure I-3. In performing deconvolution analyses, the ground surface shaking level was scaled to a peak ground acceleration (PGA) of 0.25 g that would likely be the most representative PGA for licensing applications of existing power plant sites on the east coast. The deconvolution analyses were performed for each of the two horizontal component motions for each of the five selected sets of motions fitted to the NUREG/CR-0098 [5] spectral shape (see Table 4.2). The iterated strain-compatible shear wave velocity and damping profiles for the 10 runs were then averaged to develop the generic iterated strain-compatible shear wave velocity and damping profiles. The deconvolution analyses were then repeated using the averaged profiles to develop column base motions. Parallel to the column base motions, the corresponding soil modulus and

damping properties for all the stiff and soft soil and the upper bound rock profiles were developed for compatibility in soil parameters between deconvolution and coupled cask response models.

As discussed in the report, it is very important to cross compare the soil condition (in terms of shear wave velocity) between the parametric study and cask design applications for surface soils to make sure that the inherent coefficient of restitution be comparable. It would be intuitive to assume that the coefficient of restitution is not sensitive to deeper soil stiffnesses. Based on typical dry cask dimensions, the analysis procedure is concentrated on the soil profile at the upper 10-ft range only.

It should be noted that there are subtle differences between low-strain shear wave velocity profiles (relevant for referencing) versus the iterated strain-compatible soil profiles (used in the parametric study), as shown in Figure I-2. Rigorously speaking, cross-referencing to site-specific project cases is based on the definition of low-strain shear wave velocity profiles (from geophysical sounding in the field). However, the soil modulus (and strain-compatible shear wave velocity) needs to be adjusted for various levels of shaking in numerical analyses. The analysis team feels that maintaining full rigor regarding strain-compatibility issues would bring in unnecessary complexity and thus is not warranted within the range of uncertainty on the overall problem. Furthermore, differences between the low-strain and the iterated shear wave velocity (modulus) profiles are rather small (less than 10 percent), as evidenced in Figure I-2. The rationale behind this observation is that the free stress boundary condition for the ground surface would inherently ensure relatively small shearing strains near the ground surface. To avoid any unnecessary confusion, the iterated shear wave velocity profile has been documented in Figure 3.5 and can be used for cross comparison in cask design applications.

It is important to point out that soil properties would have an insignificant role in defining ground motion shaking levels because of the inherent procedure for calibrating shaking at the ground surface reference point. For this reason, and also to minimize confusion, it has been elected to utilize the same soil profiles (iterated for 0.25 g ground shaking) for cask response analyses for different parametric PGA response cases, including PGA at 0.6 g, 1.0 g and 1.25 g, without repeating iterative solutions for other shaking levels. Cask response solutions at higher levels of ground shaking are merely intended to appreciate potential cask response qualitatively. These high ground motion levels would very unlikely be encountered in licensing situations. In addition, it is well known that the strain-compatible soil properties shown in Figure I-3 along with standard site response analysis procedures work well only to moderate levels of ground shaking. The conventional site response procedure starts to deteriorate at higher ground shaking levels and can result in unrealistic ground motions. In most projects in California, subjective judgmental modifications of the strain-compatible property procedures would be required on project specific basis, which would be difficult to implement for the parametric cask response study without defining the true site-specific soil conditions.

Besides the site soil profiles, there is a need to provide information for an upper bound soil stiffness case. It has been elected to use a stiffer soil stiffness (higher shear wave velocity) profile above the upper bound range recommended by the 1989 EPRI report [2], as shown in Figure I-1, so that the profile can cover even the rock site cases. Since the cask response solutions indicate higher cask responses for stiffer soil profiles, the adopted profile can provide a bounding case. Figure 3.5 in the report summarized the three parametric soil profiles adopted in the parametric response study. It can be observed from this figure that the chosen shear wave velocity value of 5,000 fps would be sufficiently high to cover the very stiff rock found at the eastern United States. However, softening of the rock at the ground surface would be very prevalent and likely be encountered at almost all rock sites. In addition, most cask design contractors appear to favor overlaying the rock surface by a thin layer of engineering fill. Therefore, the rock site profile at the upper 10-ft layer has been modified to reflect the expected conditions to ensure that the analysis model would capture the proper coefficient of restitution.

## References

1. Lam, Ignatius Po, H.Law, and C. T. Yang. "Modeling of Seismic Wave Scattering on Pile Group and Caissons." Report submitted to MCEER, February 25, 2004.
2. Electric Power Research Institute (EPRI). "Probabilistic Seismic Hazard Evaluations at Nuclear Plant Sites in the Central and Eastern United States: Resolution of the Charleston Earthquake Issue," Special Report, NP-6395-D, Research Project P101-53. EPRI: Palo Altos, CA. April 1989.
3. Electric Power Research Institute (EPRI). "Guidelines for Determining Design Basis Ground Motions," Final Report, EPRI TR-102293. EPRI: Palo Altos, CA. November 1993.
4. Idriss, I. M. and J. I. Sun. User's Manual for SHAKE91, "A Computer Program for Conducting Equivalent Linear Seismic Response Analysis of Horizontally Layered Soil Deposits." Program modified based on the original SHAKE program published in December 1972 by Schnabel, Lysmer, and Seed. University of California, Davis: Davis, CA. November 1992.
5. Newmark, N. M. and W. J. Hall. NUREG/CR-0098, "Development of Criteria for Seismic Review of Selected Nuclear Power Plants." U.S. Nuclear Regulatory Commission: Washington D.C. May 1978.

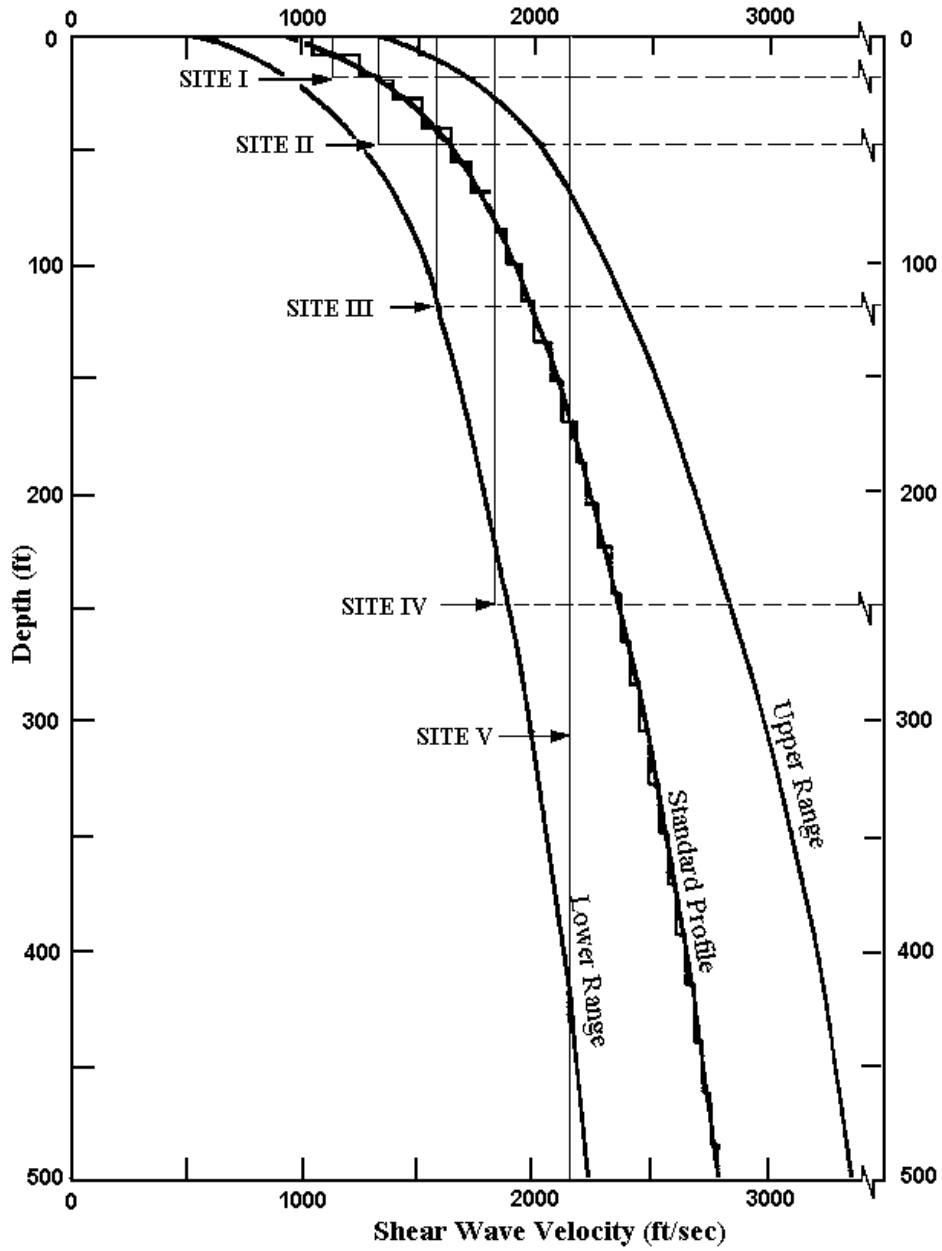


Figure I-1: Typical Shear Wave Velocity Profiles for Nuclear Power Plant Sites

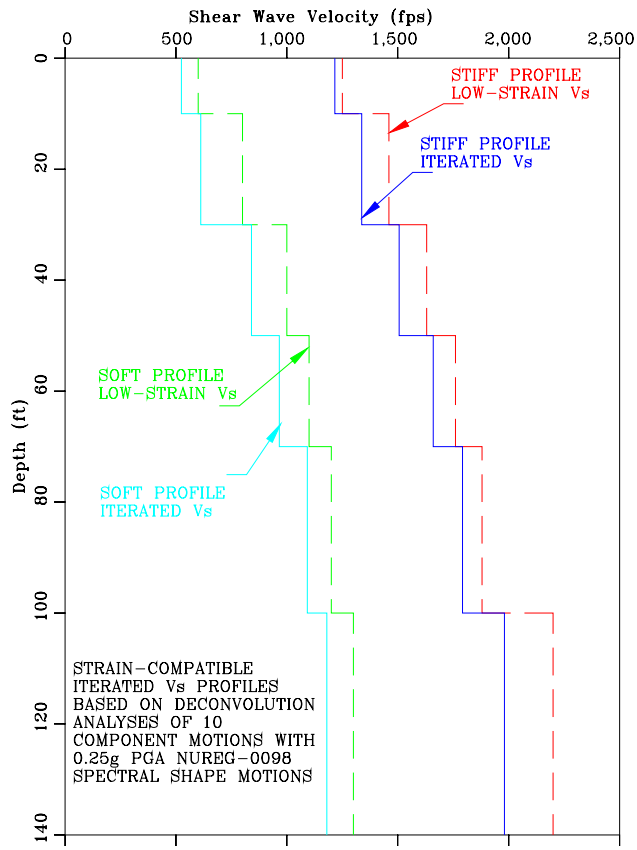


Figure I-2: Shear Wave Velocity Profiles for Soil Sites in Parametric Analyses

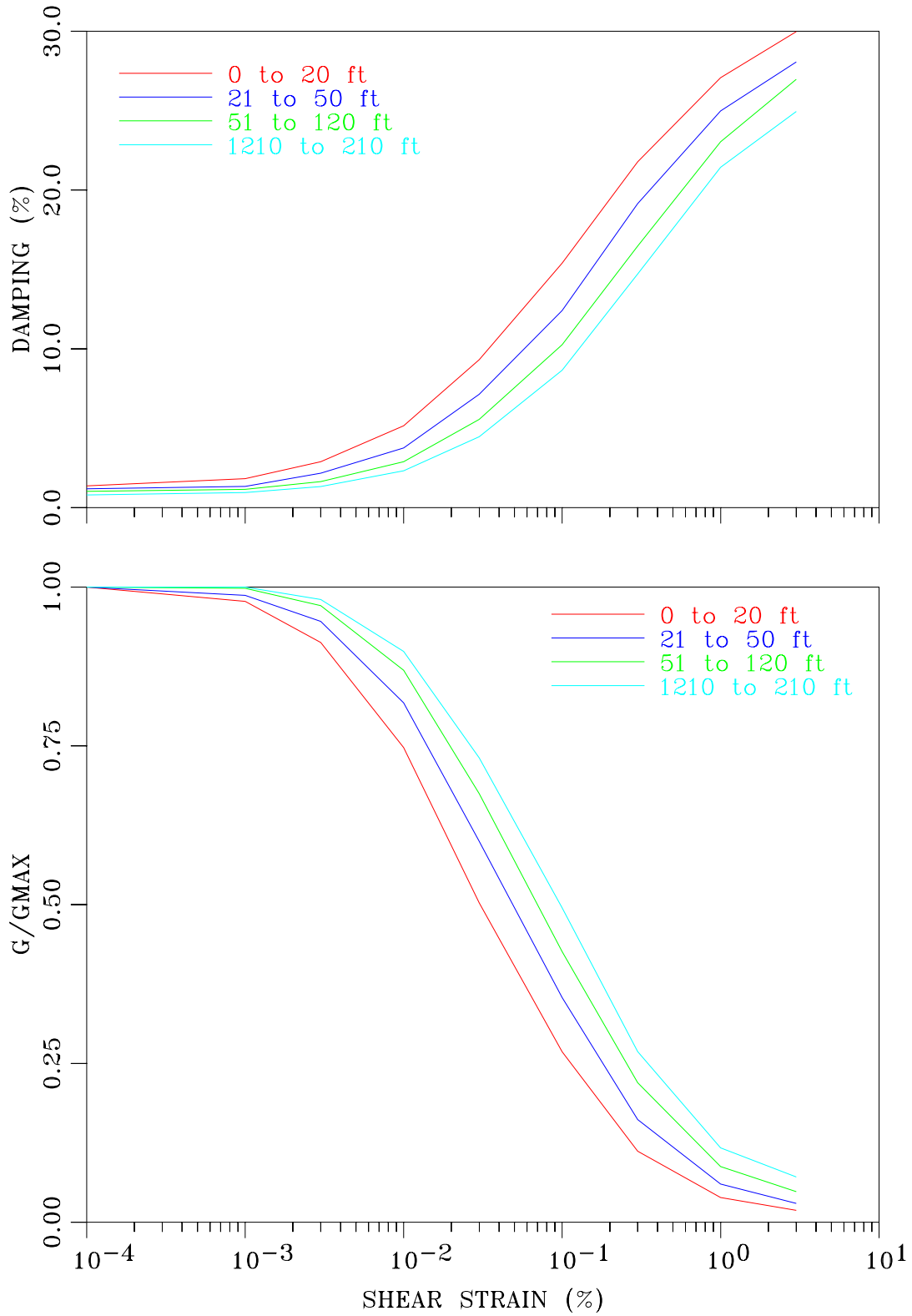


Figure I-3: Strain Compatible Soil Properties in Deconvolution Analyses



## **Appendix II: Verification of Time-Domain Wave Propagation and Various Wave-Propagation Sensitivity Studies**

INTENTIONALLY LEFT BLANK

## **Appendix II: Verification of Time-Domain Wave Propagation and Various Wave-Propagation Sensitivity Studies**

This appendix was extracted from Section 3 of a more complete report entitled *Modeling of Seismic Wave Scattering on Pile Group and Caisson* by Ignatius Po Lam, Hubert Law and Chien-Tai Yang, funded by the Multidisciplinary Center for Earthquake Engineering Research (MCEER) at the University of New York at Buffalo, through a grant from the FHWA (FHWA Contract Number DTFH61-92-C-00112). This report was submitted to MCEER on February 25, 2004 and is currently under review for publication.

Section 3 of the cited MCEER report addresses the issue of using a time-domain numerical method for conducting the classical one-dimensional site response analysis. This section is presented in this appendix to summarize some of the major background information relevant for the dry cask response problem. Other sections of the MCEER report, not included as part of this current report, includes comparing time-domain two-dimensional wave scattering of embedded foundation systems to SASSI [1] solutions.

### **II.1 One-Dimensional Site Response**

When a seismologist develops a reference rock motion, it usually represents an outcrop motion. The rock outcrop motion is employed in a one-dimensional site response program (e.g., SHAKE91 [2]) to compute free-field motions for subsequent studies required for foundation designs. Consistent with the definition of the outcrop motion, the input acceleration to SHAKE91 must be treated as ‘outcrop’ motion, not as ‘within’ motion. By treating as ‘outcrop’, the layer below the boundary where the outcrop motion is specified becomes infinite space, eliminating the potential for wave reflection/refraction at the boundary.

When the input motion to SHAKE91 is used as ‘within’ motion, the boundary is treated as a rigid base resulting in ‘prescribed motion’ at the base of the soil column. Consequently, if the input rock motion intended for ‘outcrop’ is used as ‘within’ motion in SHAKE91, overly conservative and sometimes erroneous solutions are obtained. This is a result of wave trapping within the soil deposit. Unfortunately, some practicing geotechnical engineers do not recognize these mechanics and continue to make these mistakes not only in SHAKE91 but also in other site response analysis programs.

There are cases where seismologists define a reference motion at the ground surface, especially where rock-like material cannot be located within a reasonable depth (e.g., within 200 feet). In this situation, they rely on soil attenuation relationships based on recorded surface motions to establish the reference motions at the ground surface. Depth-varying free-field motions can be computed from the reference surface motion by conducting a deconvolution analysis with the program SHAKE91. The deconvoluted motion at any depth may be requested as ‘outcrop’ or ‘within’ motion.

For the purpose of this research, we consider hypothetical soil strata, as illustrated in Figure II-1 showing the material properties assigned to each soil stratum. The reference motions chosen for this study are at the ground surface; Figures II-2 and II-3 present the characteristics of the reference motions in two directions, horizontal and vertical, defined at the ground surface. These motions have been spectrum-matched to certain design response spectra. Given the reference motions defined at the surface, deconvolution analyses were conducted to compute the free-field motions at every soil layer as ‘within’ motion, while the bottommost layer is requested as both ‘within’ and ‘outcrop’ motions. The free-field motions as computed from SHAKE91 are illustrated in Figures II-4 and II-5 for the horizontal and vertical directions, respectively.

Here attempts are made to reproduce the SHAKE91 solutions using the ADINA [3] program. The base input acceleration to ADINA model is the ‘within’ motion at the bottommost layer computed from the deconvolution analysis using SHAKE91. The prime reason of using the SHAKE91 ‘within’ motion to excite the ADINA finite element model is that rigid base excitation is implemented without employing transmitting boundary conditions. If the solutions are correct, the surface motion computed from ADINA should duplicate the reference surface motion.

Several parameters affect the ADINA solutions. To understand how they influence the numerical results, comparison between the ADINA solutions and the SHAKE91 solutions is made by performing a parametric study that addresses the following issues:

- Effects of vertical side boundaries
- Effects of time integration schemes
- Implementation of damping

## II.2 Effects of Vertical Side Boundaries

A two-dimensional finite element method is used to simulate the one-dimensional wave propagation in order to investigate the effectiveness of various side boundary conditions. The finite element domain representing the same layered soils used in SHAKE91 is shown in Figure II-6. Seismic response analyses of the soil strata were performed using the following boundary conditions:

- Free side boundary
- Fixed side boundary
- Edge column boundary
- Slaving of left and right boundaries
- Transmitting side boundary

Schematics of these side boundary conditions are shown in Figure II-7.

Figure II-7 (a) is a finite element model with free side boundaries indicating no constraint at the side boundary nodes. These side boundary nodes are free to move in any direction.

Figure II-7 (b) illustrates a finite element model with fixed side boundaries implying that no vertical and horizontal movement relative to the base is allowed at the two side boundaries.

Figure II-7 (c) represents a model with two edge columns at the side boundaries where two corresponding nodes of the soil column at same elevations are slaved together. The intent is to create shear beam columns near the boundaries.

Figure II-7 (d) is an illustration of how one-dimensional wave propagation is modeled by means of slaving the leftmost nodes to the rightmost nodes at the side boundaries. Slaving is done in the both directions, horizontal and vertical, such that the slaved nodes move together.

Figure II-7 (e) depicts treatment of the side boundaries using dashpots similar to those used at the base of some numerical models to represent a half space suggested by Lysmer and Kulemeyer [4].

In all the cases discussed above, rigid base excitation is the primary form of seismic loading to the ADINA finite element model. This is accomplished by assigning the ‘within’ motion computed from the SHAKE91 deconvolution analysis at the base of the soil column. Only horizontal site response behavior is assessed in this exercise (i.e., vertical motion is not included). The horizontal ground response is

computed at the surface (depth 0 ft) from each of the finite element model, and the result is compared with the reference ground motion in Figure II-8 in terms of acceleration response spectra.

It can be seen that the ground response of the fixed-side-boundary model is largely magnified by reflected waves as overly restraint conditions were imposed in the analysis. The free side boundaries also yield a superfluous response that is not satisfactory as compared to the reference surface motion. Although free or fixed boundary condition is typically available in general finite element codes, neither could provide accurate ground response simulating one-dimensional wave propagation.

The finite element with dashpot side boundary also yields unsatisfactory ground response. However Lysmer and Kulemeyer report the effectiveness of the dashpot concept when used at the base representing the half space to absorb seismic energy, and the efficiency of absorbing energy decreases largely with the increase of the incident angle. The efficiency is about 95% for a zero incident angle but reduces to around 10% for a 30-degree incident angle. However, no discussion is found for the dashpot concept being used at the side boundary. Based on the result obtained from this study, the dashpot concept applied at the side boundaries is not very effective in modeling the one-dimensional shear beam problem. Perhaps the side boundary where the dashpots are attached is too close to the center of the finite element. Of course, if the side boundaries are moved 'far' away from the centerline of the model, the solutions would converge to the one-dimensional situation regardless of the type of boundary.

The solution of the model with a two-edge column concept shows a reasonable degree of accuracy as compared to the benchmark surface motion. In this model, the width of edge column is 61 feet. It is anticipated that width of the edge columns might influence the solutions, and its effects will be discussed later.

The response for the finite element model, which slaves the leftmost nodes to the rightmost nodes converges very close to the benchmark surface motion, and the model appears to be the most suitable for simulating a simple shear beam theory. While this boundary condition can be used for simple models where the left side and right side of the finite element mesh have similar geometric configurations and properties, it would not be suitable if the two sides have different ground elevations, such as retaining walls or sloping ground conditions.

For these parametric studies, it appears that the edge column concept and the slaving left-and-right boundary concept show promising results that can be used for general application depending on situations. To further examine the results, the depth varying motions from these two models are compared with SHAKE91 depth-varying motions, as shown in Figures II-9 and II-10.

## **II.2.1 Effects of Edge Column Widths**

As discussed earlier, the technique of slaving the leftmost nodes to the rightmost nodes is not always suitable for all the geotechnical problems, such as situations where there is a retaining wall, wharf structure or sloping ground. In these cases, the edge column concept may be used. To use two edge columns for general application, it is necessary to understand the effects of edge column widths. For this report different edge column widths were considered while keeping the distance to the boundary from the centerline of the model unchanged.

In this sensitivity analysis, we elect to use the same hypothetical soil strata as shown in Figure II-1, which has a total thickness of 185 ft. The side boundaries are 246 ft away from the centerline of the model. Each of the side boundaries is attached to an edge column with varying widths, as shown in Figure II-11. The following edge column widths were considered:

- Edge Column Width =  $1/6 H$
- Edge Column Width =  $1/3 H$
- Edge Column Width =  $2/3 H$
- Edge Column Width =  $H$

where  $H$  is the thickness of the ground. The solutions with different column widths are provided in Figure II-12. When compared to the benchmark surface motion, closer agreements are obtained with the increase of edge column widths. One can imagine that a narrower edge column tends to behave more like a free side boundary, and that a wider edge column approaches to a shear beam model when only horizontal excitation is considered.

In theory, the solutions of the model with a sufficiently wide edge column should approach to the response of the free field motions derived from a shear beam model under horizontal excitation. However, it becomes a tradeoff between the finite element size (or the computing time) and the accuracy. For practical purposes in most bridge engineering applications, a minimum edge column width should be  $1/3 H$  or larger in order to obtain reasonable structural responses beyond 0.5-sec periods. It would be desirable to perform sensitivity analyses, like the one presented here, using site specific soil conditions prior to performing actual designs.

## II.2.2 Effects of Distances to the Boundary

In the preceding section, the effect of edge column width is evaluated while keeping the distance to the side boundary from the centerline of the model unchanged. In addition to the edge column width, the solutions would also depend on proximity to the side boundary. The sensitivity analyses were performed by varying the distance to the side boundary but maintaining the edge column width to  $1/3 H$ . The following side boundary distances were evaluated:

- Distance to Side Boundary =  $1.2 H$
- Distance to Side Boundary =  $1.5 H$
- Distance to Side Boundary =  $1.8 H$

where  $H$  is the thickness of the ground. We consider these distances to be within a practical range for most design applications. Figure II-13 shows comparison of surface motions from the three models with increasing distances to the side boundary. It appears that the solutions are not very sensitive to the distance to the boundary in this study. However, it is not advisable to have the side boundaries too close to the centerline.

## II.2.3 Effects of Time Integration Schemes

In the time domain schemes as employed by ADINA and other computer codes, the differential equations are solved using a numerical step-by-step integration procedure. Several integration schemes are available based on different interpolations between displacements, velocity and acceleration, as well as the time step of the equilibrium established [5]. The following integration schemes were investigated:

- Wilson's  $\theta$  Method
- Newmark Method ( $\delta = 0.5$  and  $\alpha = 0.25$ )
- Newmark Method ( $\delta = 0.65$  and  $\alpha = 0.331$ )

Figure II-14 shows results of three different integration schemes for the model with the edge column concept. The responses vary with the different time integration schemes; however the difference is obvious only in a high frequency range. For practicality, any of the time integration methods is considered acceptable.

## II.2.4 Treatment of Rayleigh Damping

Perhaps the greatest difference between SHAKE91 and ADINA is the treatment of damping in the respective numerical procedures. The frequency response function computed within SHAKE91 uses a damping ratio, which is frequency independent. This will result in constant energy dissipation across the spectrum. However, most finite element programs including ADINA employ a Rayleigh damping concept, which would lead to frequency dependent damping characteristics. When using Rayleigh damping for dynamic analyses, it is possible to adopt one of the following procedures:

- Mass proportional damping only ( $\alpha$ )
- Stiffness proportional damping only ( $\beta$ )
- Both mass and stiffness proportional damping ( $\alpha$  and  $\beta$ )

Because the damping values vary with frequency in the Rayleigh damping concept, it is necessary to anchor the desired damping ratio at a specific frequency, e.g., the vibration period of the system. For the mass proportional damping or stiffness proportional damping, only one anchoring point can be selected. When mass and stiffness proportional damping is used, two anchoring points must be chosen.

For a general case where both mass and stiffness related damping is used, the coefficients  $\alpha$  and  $\beta$  can be determined from

$$\alpha + \beta \omega_i^2 = 2 \omega_i \xi_i$$

where  $\xi_i$  is damping ratio at angular frequency  $\omega_i$ . The relationship requires two frequencies to solve both coefficients ( $\alpha$ ,  $\beta$ ). If mass proportional damping is used, then the coefficient  $\alpha$  is determined as

$$\alpha = 2 \omega_i \xi_i$$

When stiffness proportional damping is used, the coefficient becomes

$$\beta = 2 \xi_i / \omega_i$$

Sensitivity analyses were conducted using the three different Rayleigh damping methods; all were calibrated to the same damping ratio used in SHAKE91. Using mass and stiffness proportional damping could offer more flexible means of calibrating the damping ratio. Table II-1 tabulates Rayleigh damping parameters for each case, and Figure II-15 shows the results of the sensitivity analyses. Note that the finite element mesh with the left and right boundaries slaved together was employed. From comparison among the solutions resulting from different implementation of the damping parameters, it appears that all the methods offer reasonable solutions.

## II.3 Two Component Motions

So far, horizontal motion is the only base excitation accounted for in the finite element analyses, and thus the response can be checked against the behavior of vertically propagating shear waves that can be treated

with a classical shear beam theory. However, most seismic designs consider earthquake loading in two or three directions. To implement two component motions in the finite element model, the reference vertical motion defined at the ground surface requires deconvolution in order to obtain the input base motion; this was accomplished with SHAKE91. The ADINA finite element model is then excited with the vertical and horizontal motions simultaneously. The material properties used in ADINA are based on linearly elastic continua adhering to general Hooke's law where Young's modulus (E) and shear modulus (G) are related through Poisson's ratio ( $\nu$ ) such that

$$E = 2(1+\nu)G$$

In practice however when computing depth varying horizontal and vertical motions with SHAKE91, separate computer runs are made; one with S-wave velocity (Shear Modulus) profile, and one with P-wave (Constraint Modulus) profile. Often, a few iterations are performed within SHAKE91 to achieve strain compatible moduli, and it is carried out separately for the horizontal direction and vertical direction. The iteration process could result in incompatibility between S-wave and P-wave velocities. If the iterative solutions are adopted in SHAKE91, it is difficult to compromise the comparison between SHAKE91 and ADINA.

In order to reconcile results of two-component shaking from ADINA with those of SHAKE91, one must verify that the P-wave velocity and S-wave velocity employed by SHAKE91 are uniquely related, similar to the general Hooke's law.

The comparison between SHAKE91 and ADINA on the two-component motion is shown in Figure I-16 using the finite element model that slaves the left boundary to the right boundary. The comparison is very favorable although there are some discrepancies in the treatment of damping. For example, SHAKE91 uses the different damping ratios in the horizontal deconvolution from the vertical deconvolution, while ADINA allows only one set of Rayleigh damping parameters that are applied to the entire system, which is excited by horizontal and vertical motions simultaneously. The Rayleigh damping used in the finite element model has been calibrated to the damping ratios of the horizontal SHAKE91 profile. Based on this observation, it seems that minor discrepancy in soil damping does not contribute to significant differences in the seismic response of the ground.

A similar comparison is made between SHAKE91 and ADINA using the two-edge column concept; the results are shown in Figure II-17. The following summarizes the ADINA model:

Distance to the side boundary from the centerline = 246 ft  
Width of the edge column = 65 ft

The ADINA solutions using the two-edge columns are not as good as those results presented in Figure II-16. Attempts were made to improve the ADINA solutions by increasing the width of the edge column; however the degree of improvement is poor. The reason is attributed to the fact that the finite element model with two-edge columns is unable to maintain the constraint conditions required in one-dimensional wave propagation especially when vertical motion is introduced. Imagine a P-wave propagation in the finite element model with two edge columns. Due to the Poisson's ratio effects, the vertical strain in soil due to passage of P-wave would lead to horizontal displacement pushing the edge columns outward. This would have resulted in a violation of the constraint modulus assumption made in SHAKE91 for the vertical wave propagation problem.

To make this point, site response analysis was performed using the vertical input motion only, and snapshots of relative deformation profiles of the two edge boundaries are plotted in Figure II-18. Without horizontal excitation, the edge boundaries deform laterally as a result of the Poisson's effect. If a true



one-dimensional condition is maintained, the two side boundaries would have moved together, and the profiles of the two edge columns would have been identical. From inspection of the edge boundary profiles, it is obvious that the two-edge column model tends to deviate from one-dimensional behavior when the vertical motion is introduced. If the vertical motion is absent, the response of the edge column model seems to yield reasonable results.

## References

1. Stevenson & Associates, Inc. "SUPER SASSI/PC User's Manual." May 1996.
2. Idriss, I. M. and J. I. Sun. User's Manual for SHAKE91, "A Computer Program for Conducting Equivalent Linear Seismic Response Analysis of Horizontally Layered Soil Deposits." Program modified based on the original SHAKE program published in December 1972 by Schnabel, Lysmer, and Seed. University of California, Davis: Davis, CA. November 1992.
3. ADINA R&D Inc. User's Guide for ADINA: Automatic Dynamic Incremental Nonlinear Analysis. MA. June 2003.
4. Lysmer, J. and Kulemeyer, R.L. "Finite Dynamic Model for Infinite Media," *Journal of Engineering Mechanics Division*. ASCE, Vol. 95, No., EM4, pp. 859-877. August 1969.
5. Bath, K-J. *Finite Element Procedures in Engineering Analysis*. Prentice-Hall Inc. 1982.

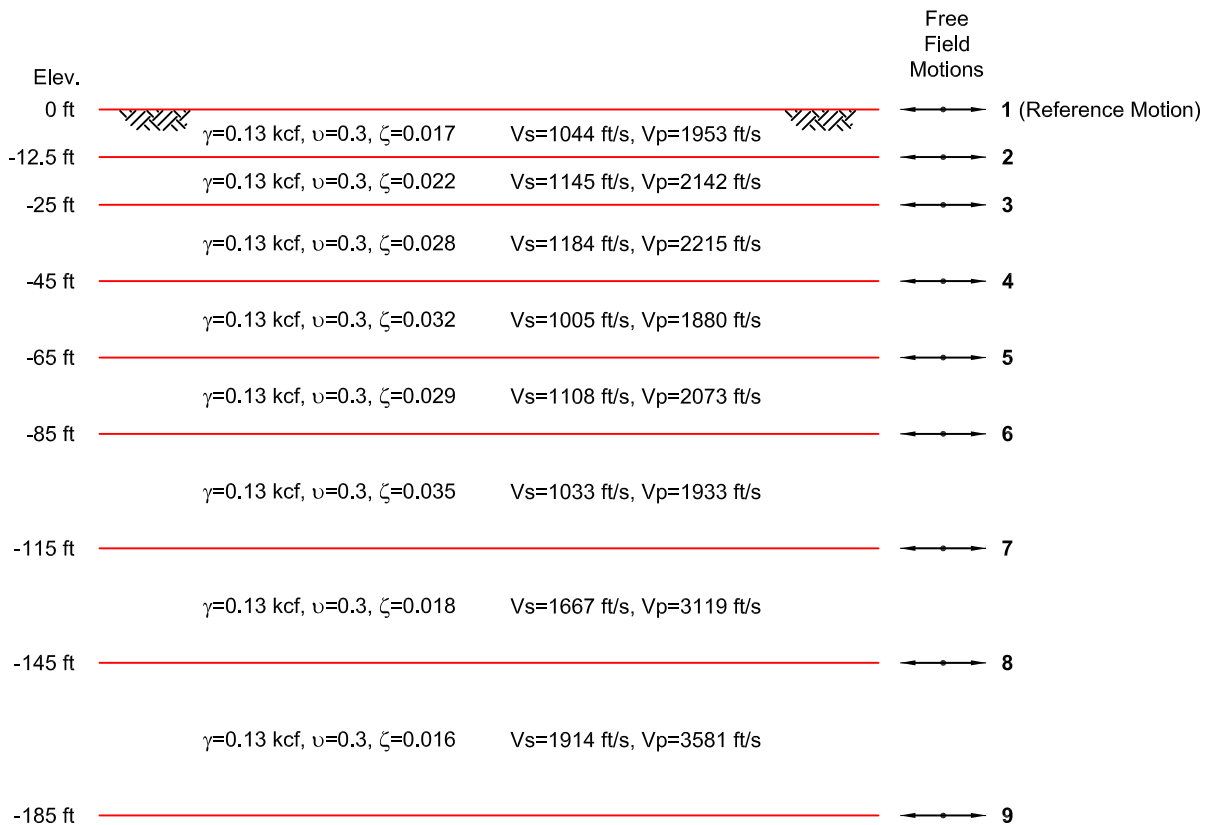


Figure II-1. Hypothetical Soil Strata

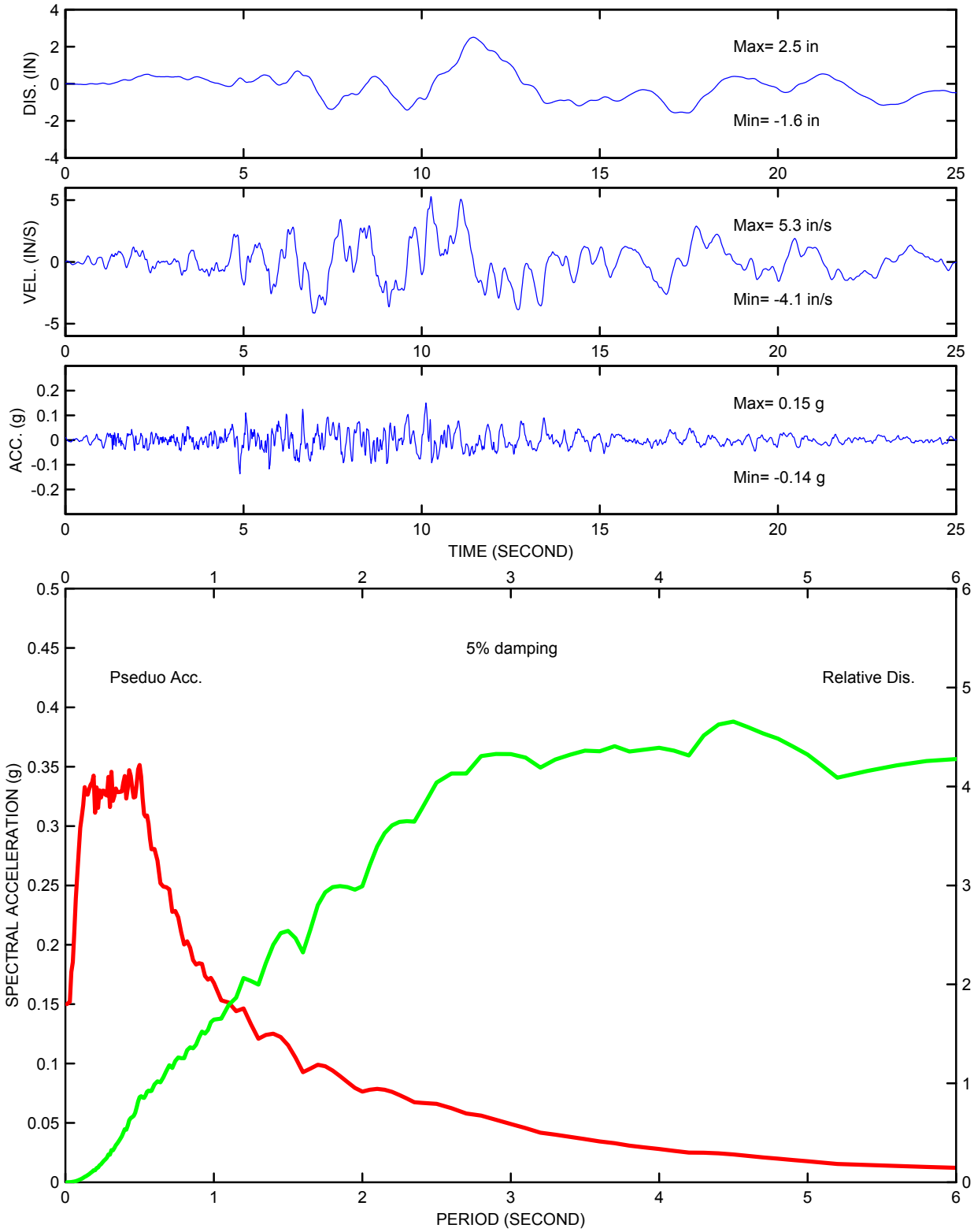


Figure II-2. Reference Horizontal Ground Motion at Surface

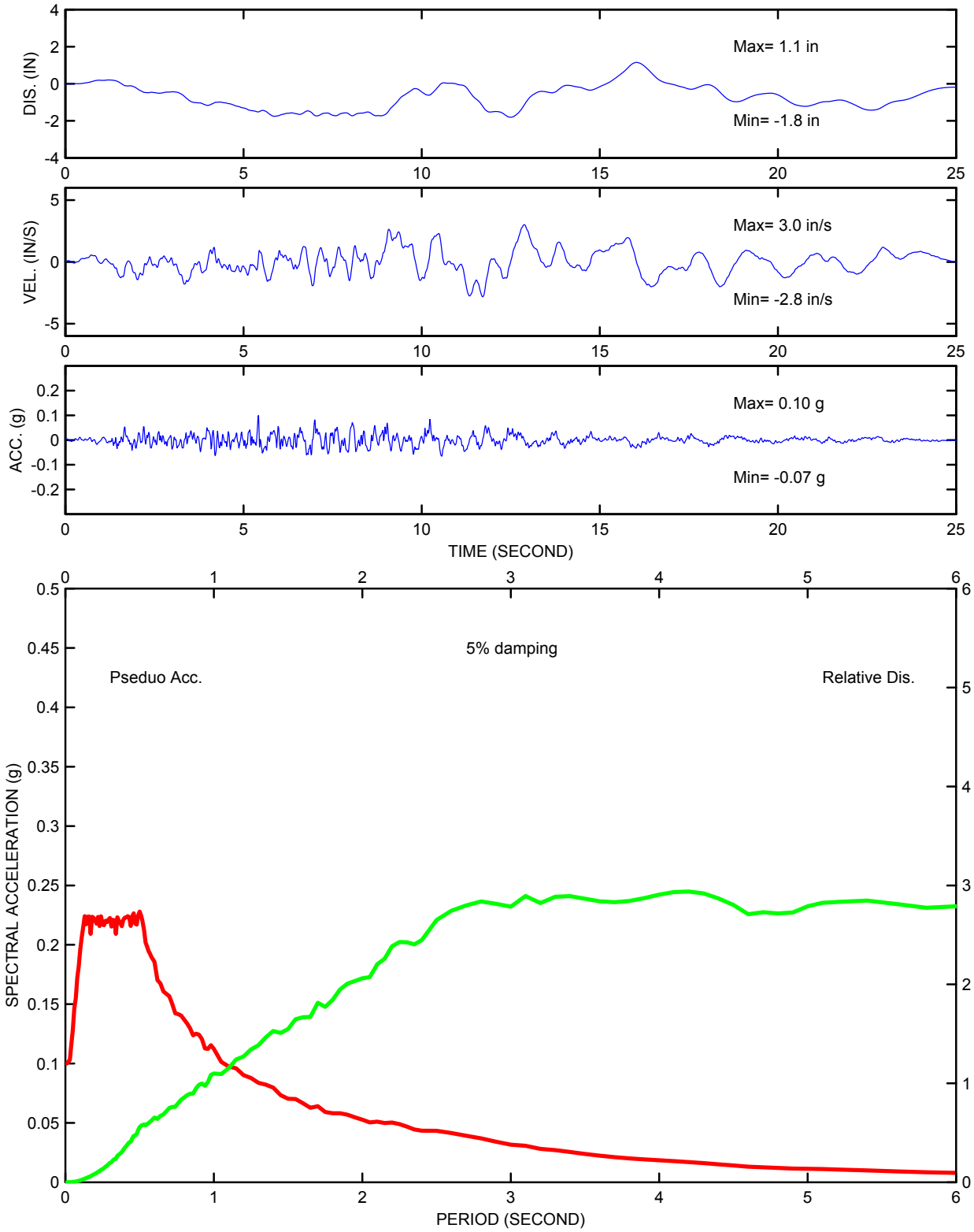


Figure II-3. Reference Vertical Ground Motion at Surface

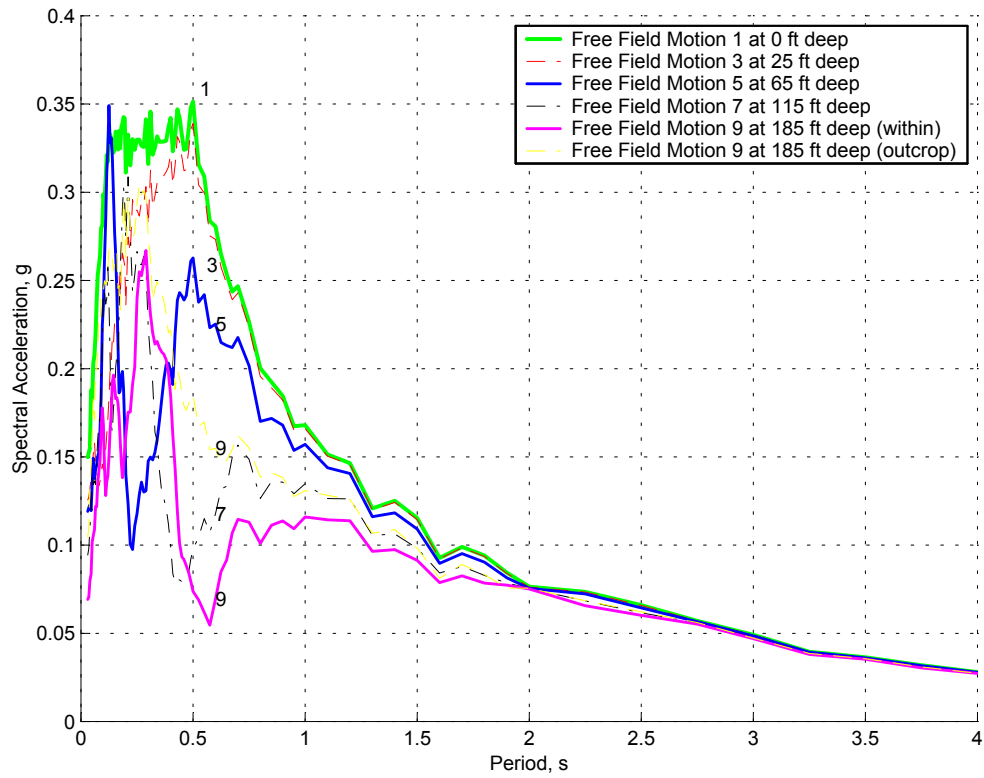


Figure II-4. Depth Varying Free Field Horizontal Motions

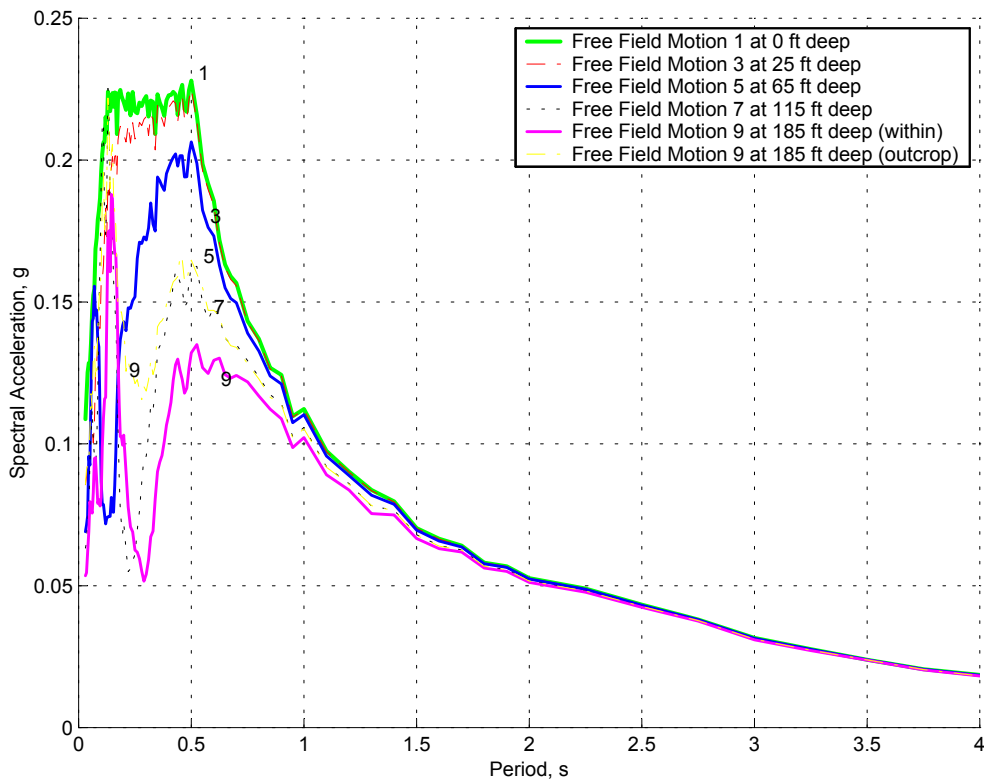


Figure II-5. Depth Varying Free Field Vertical Motions

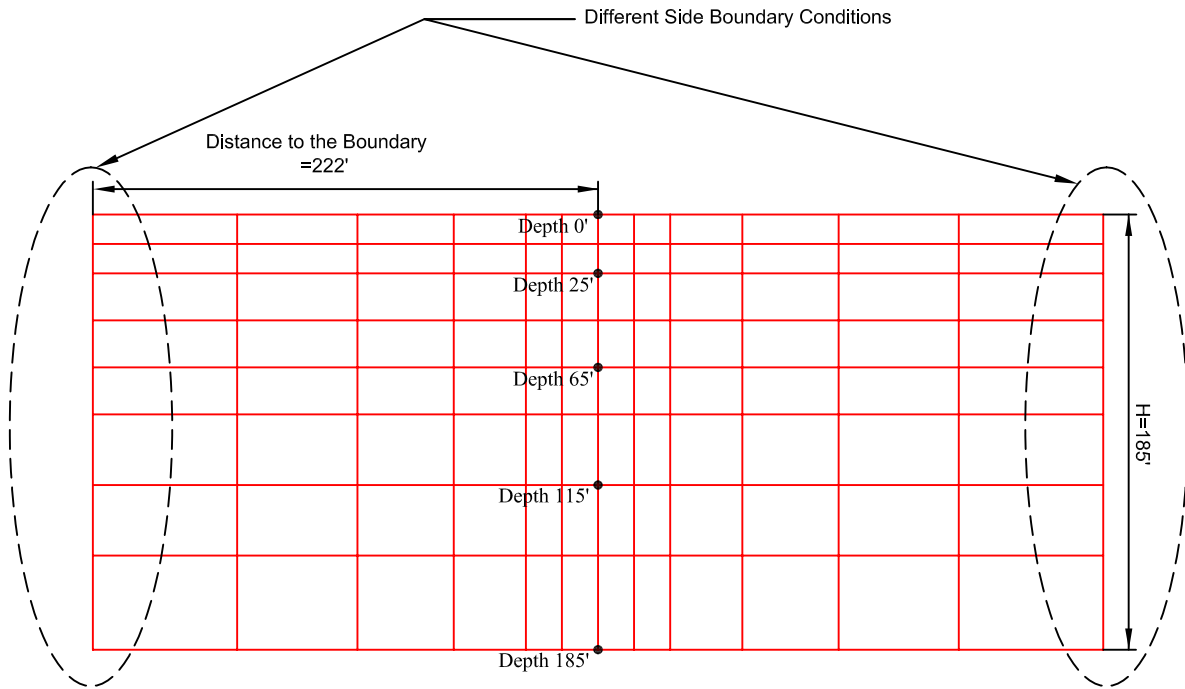
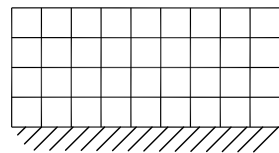
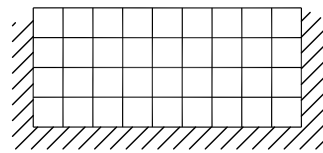


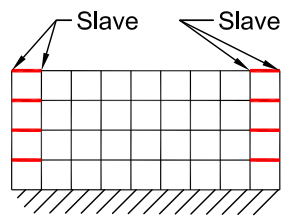
Figure II-6. Finite Element Model



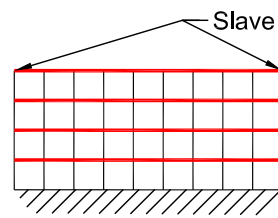
(a) Free Side Boundary



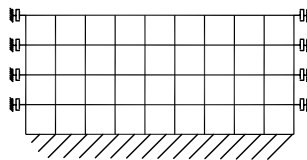
(b) Fixed Side Boundary



(c) Two Edge Columns



(d) Slave Left & Right Boundaries



(e) Transmitting Side Boundary

Figure II-7. Different Side Boundary Conditions

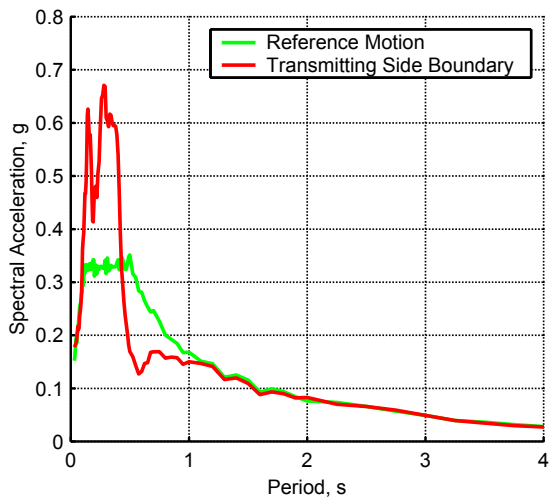
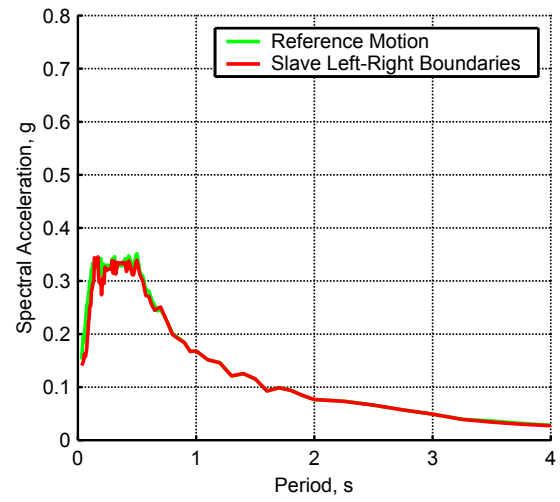
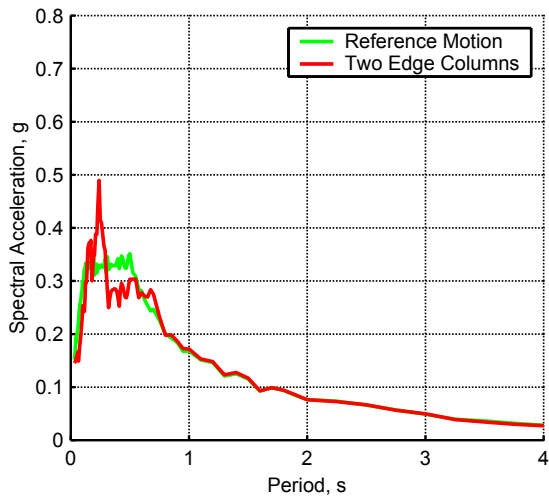
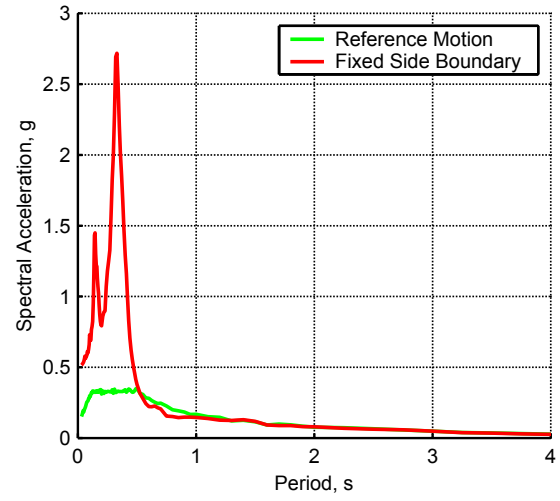
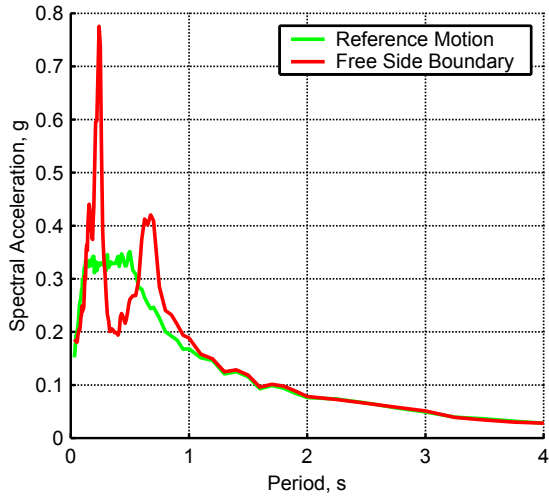


Figure II-8. Effects of Side Boundary Conditions

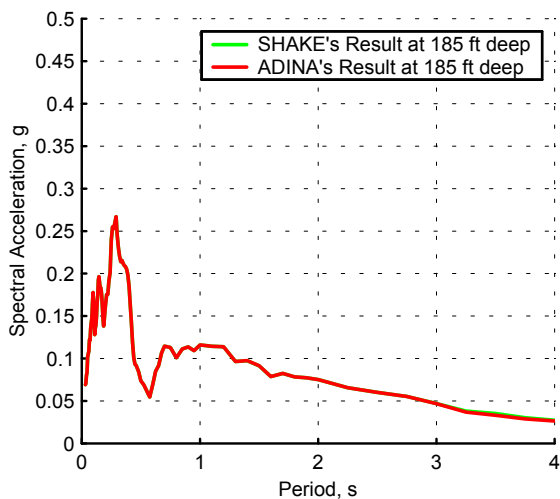
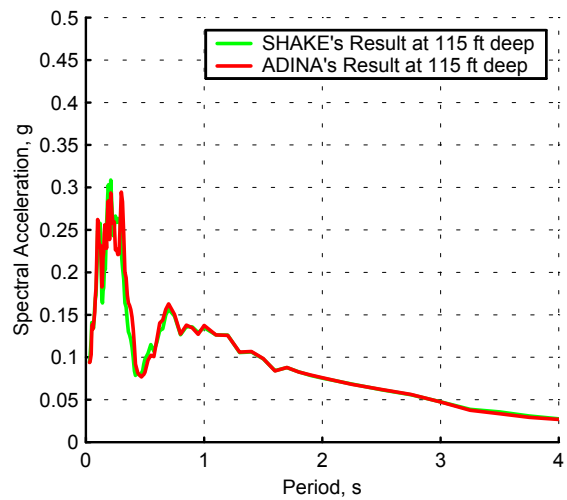
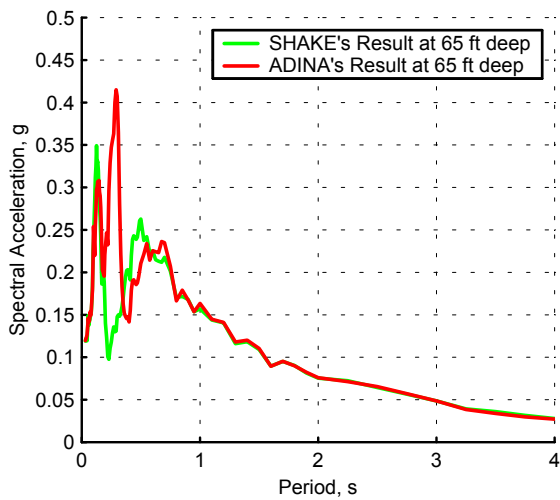
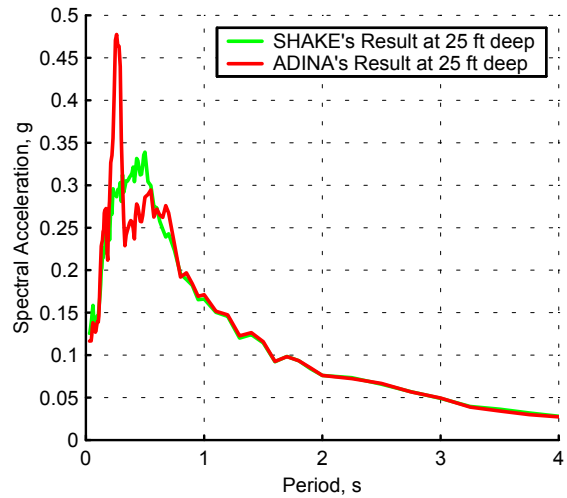
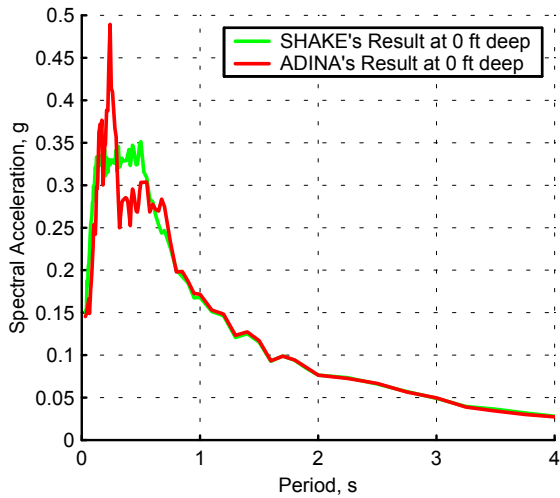


Figure II-9. Comparison of SHAKE Results and ADINA Results Of the Model with Two Edge Columns

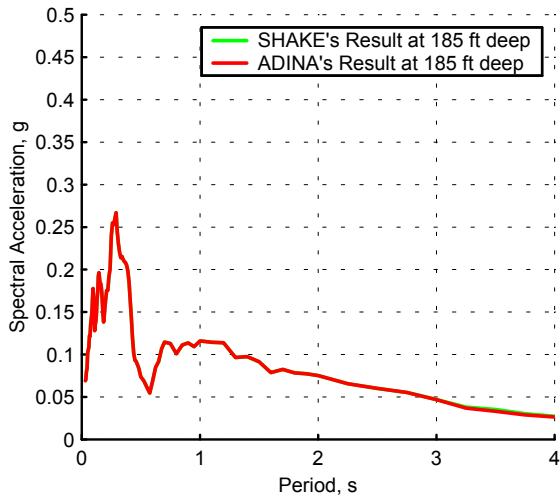
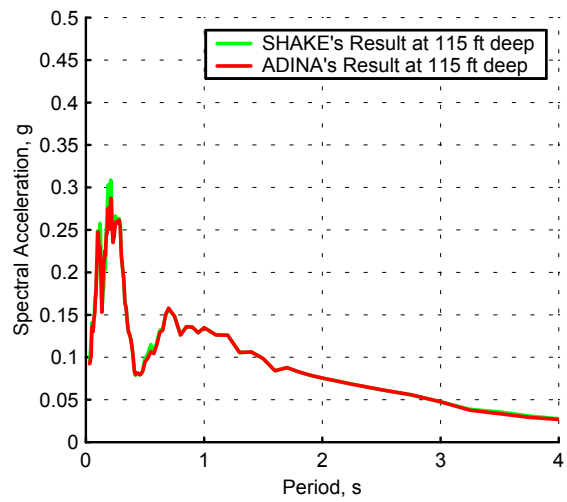
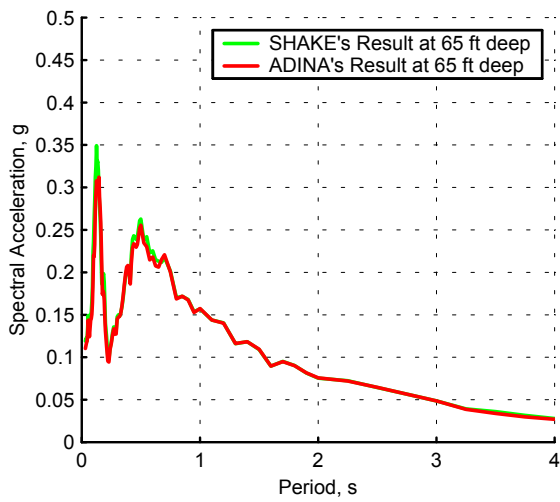
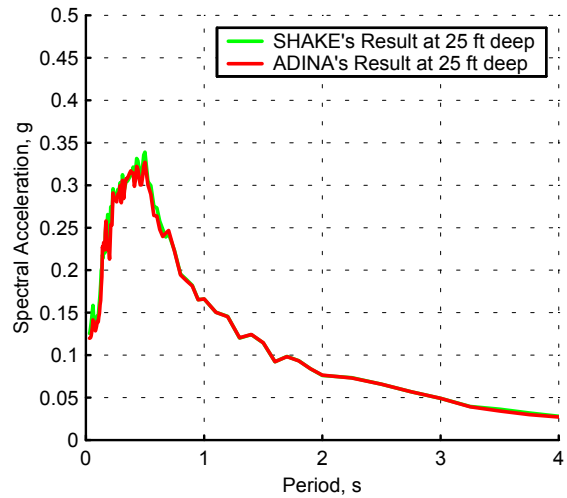
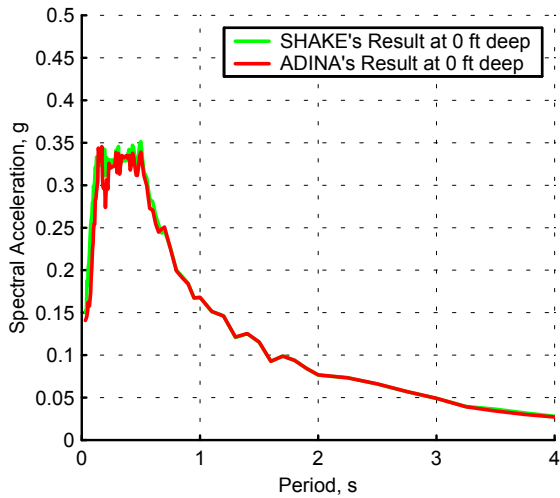


Figure II-10. Comparison of SHAKE Results and ADINA Results of the Model with Slaving Left and Right Boundaries



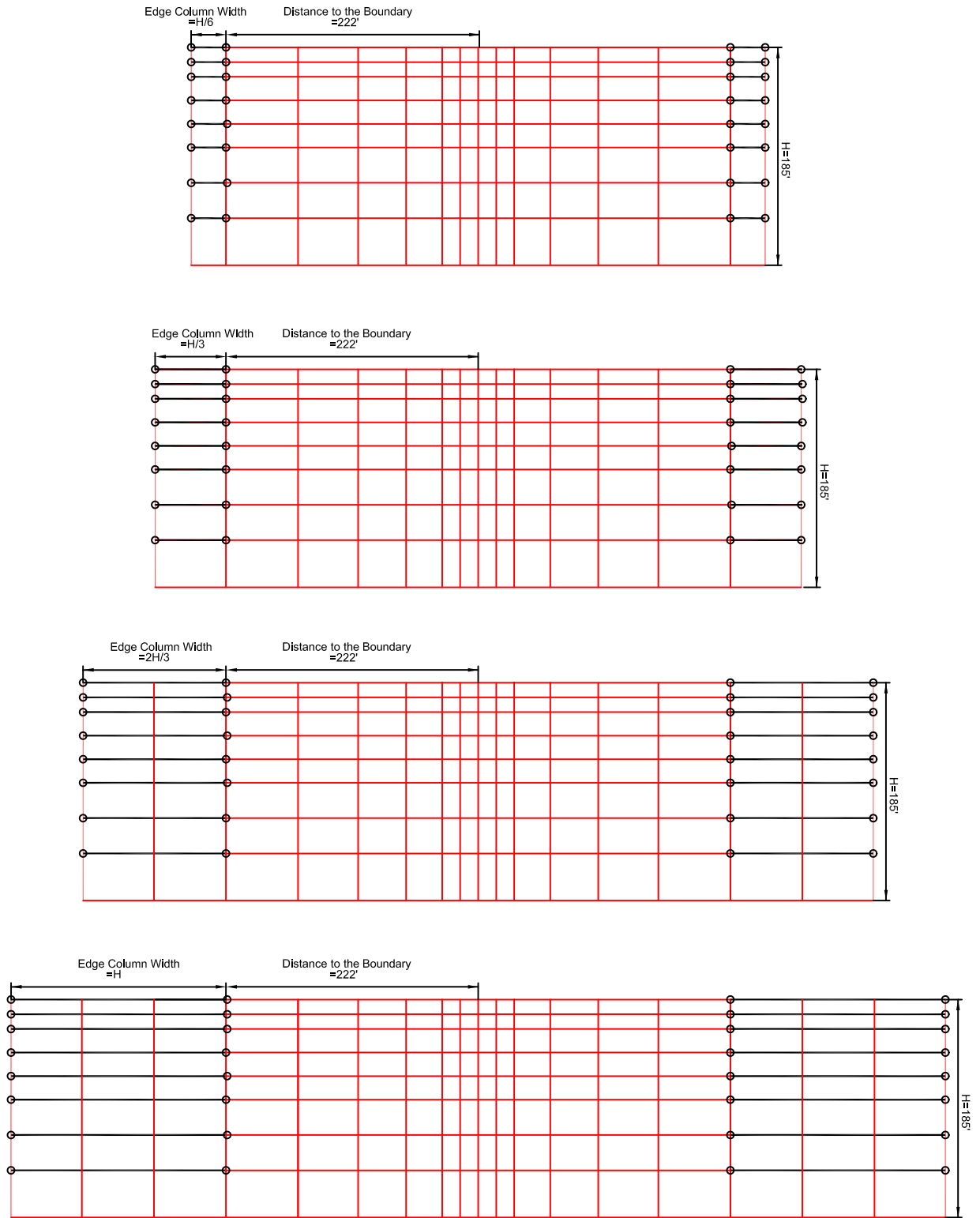


Figure II-11. FEM Model with Different Edge Column Widths

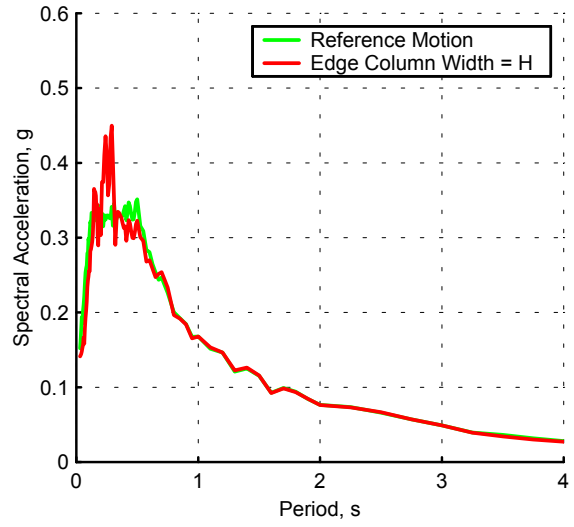
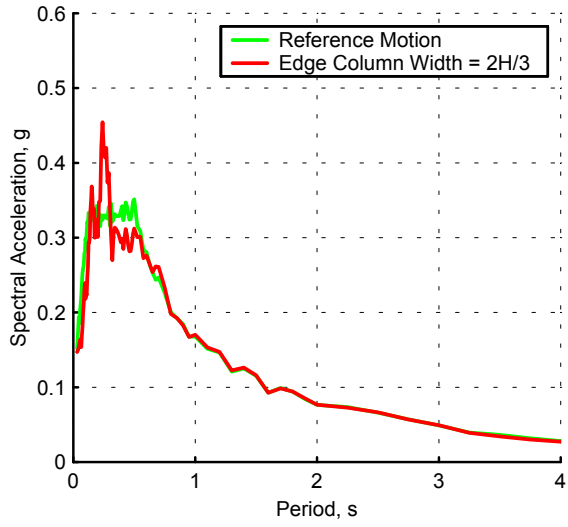
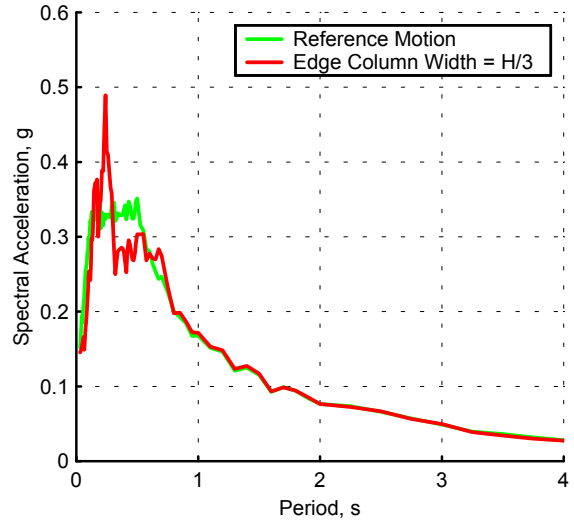
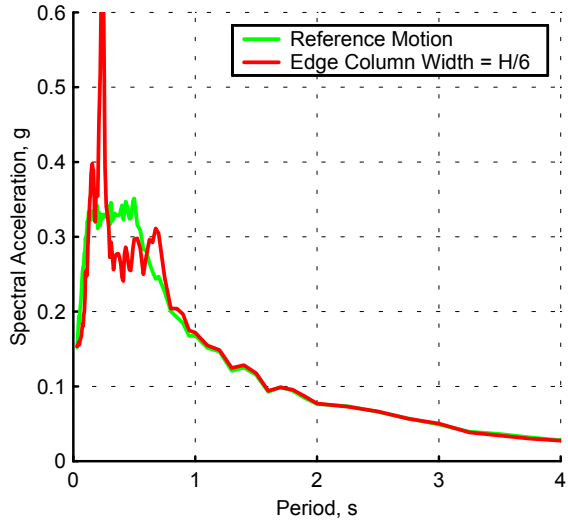


Figure II-12. Effects of Edge Column Widths

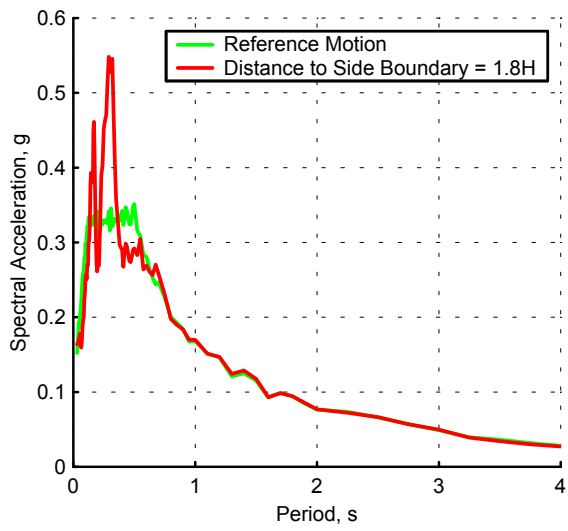
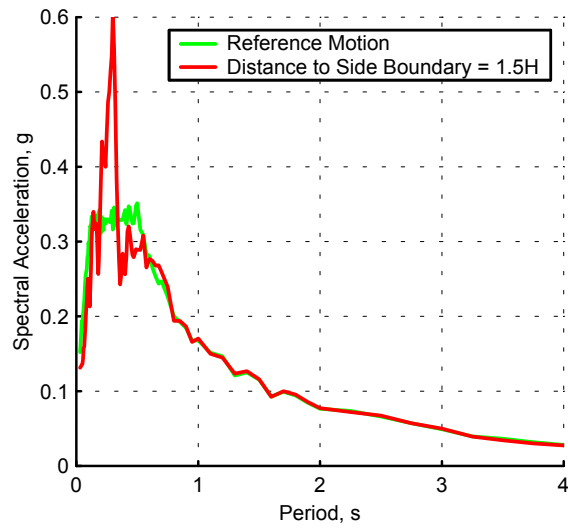
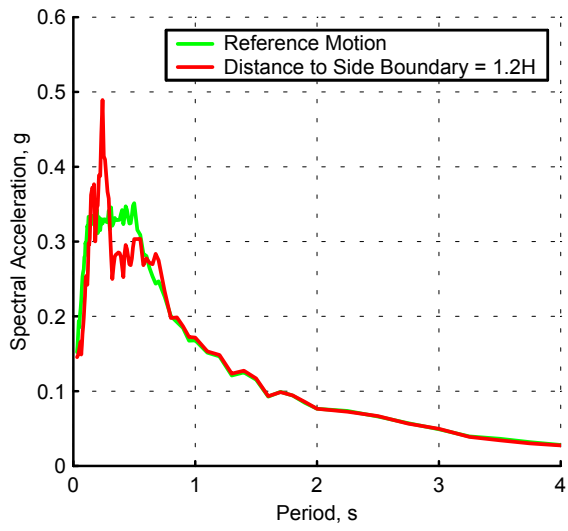


Figure II-13. Effect of Different Distance to Boundary

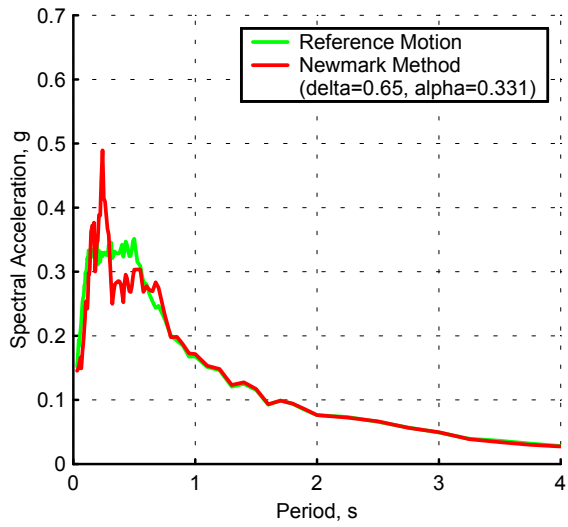
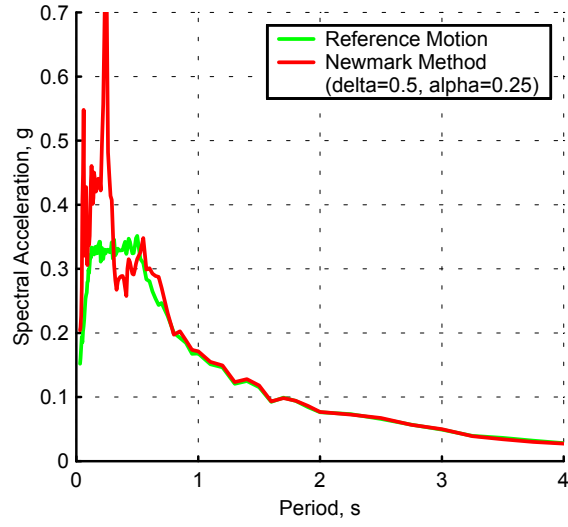
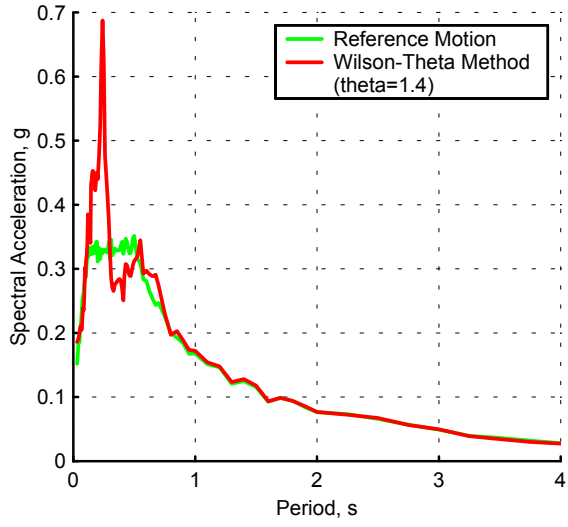


Figure II-14. Effect of Different Integration Scheme

Table II-1. Rayleigh Damping Parameters

Damping Ratio ( $\zeta$ )	Mass-Proportional Damping Only	Stiffness-Proportional Damping Only	Rayleigh Damping	
	$\alpha$	$\beta$	$\alpha$	$\beta$
0.017	0.403	0.00287	0.202	0.00143
0.022	0.522	0.00371	0.261	0.00186
0.028	0.664	0.00472	0.332	0.00236
0.032	0.759	0.00540	0.379	0.00270
0.029	0.688	0.00489	0.344	0.00245
0.035	0.830	0.00590	0.415	0.00295
0.018	0.427	0.00304	0.213	0.00152
0.016	0.379	0.00270	0.190	0.00135

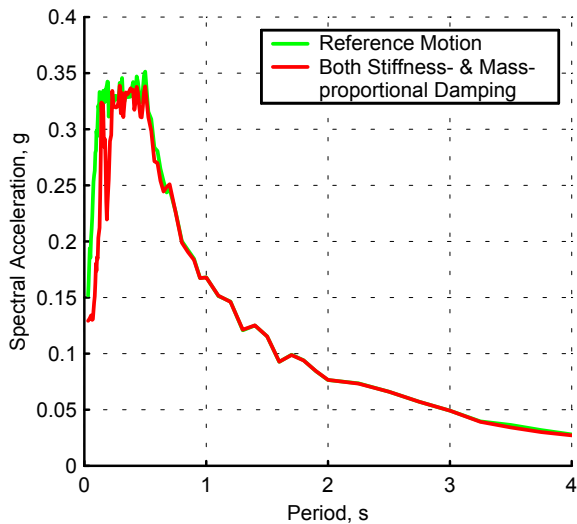
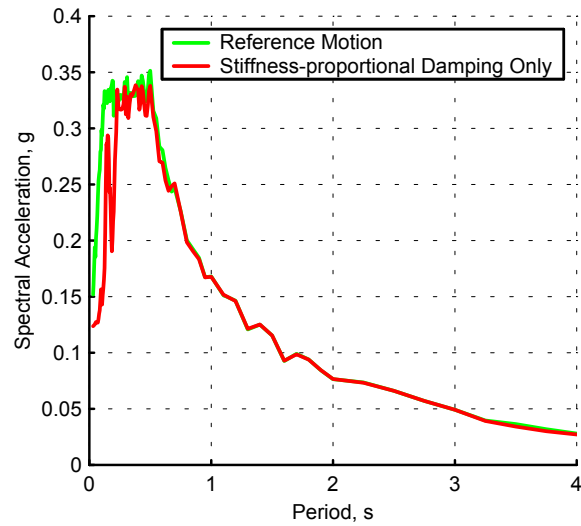
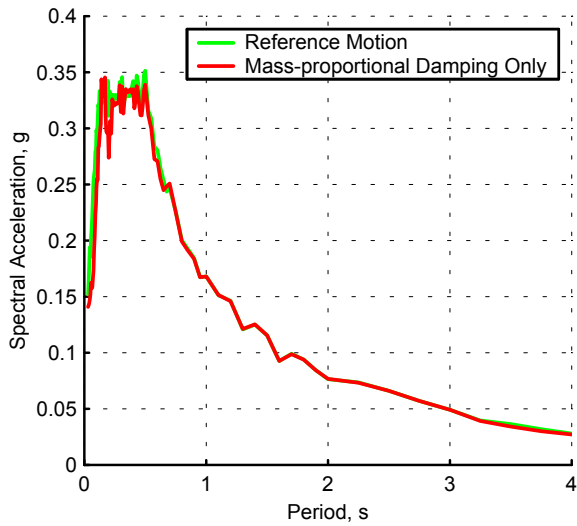


Figure II-15. Effect of Different Damping Assignments

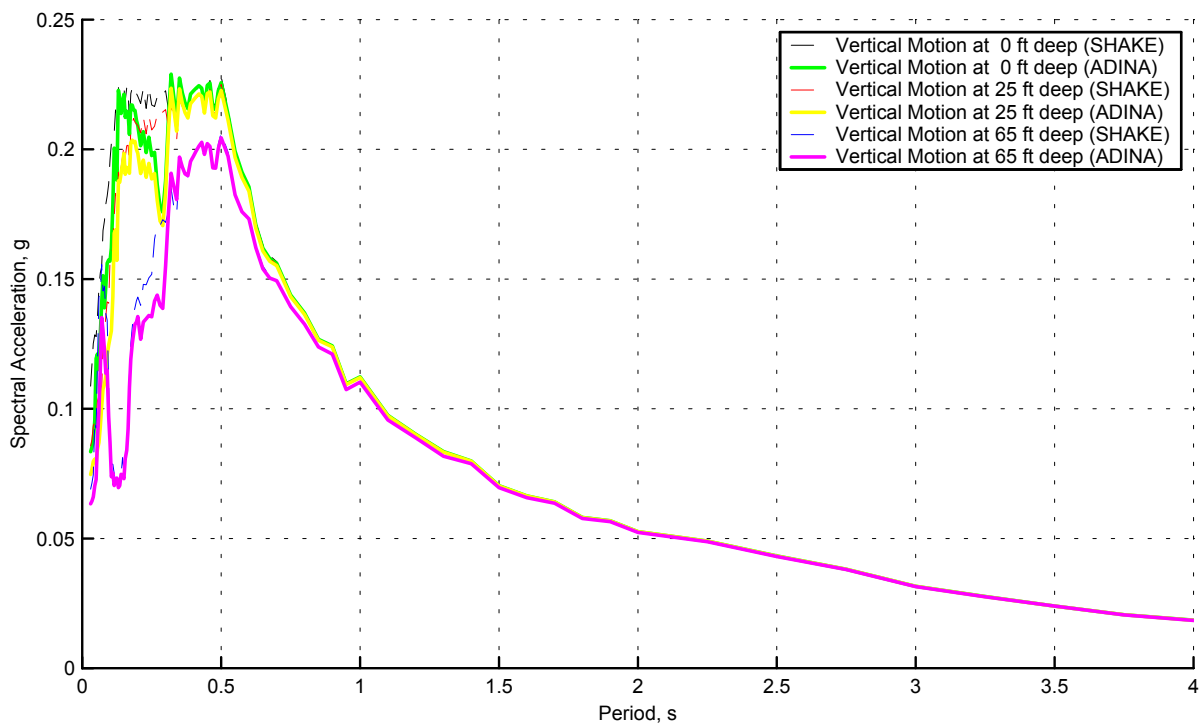
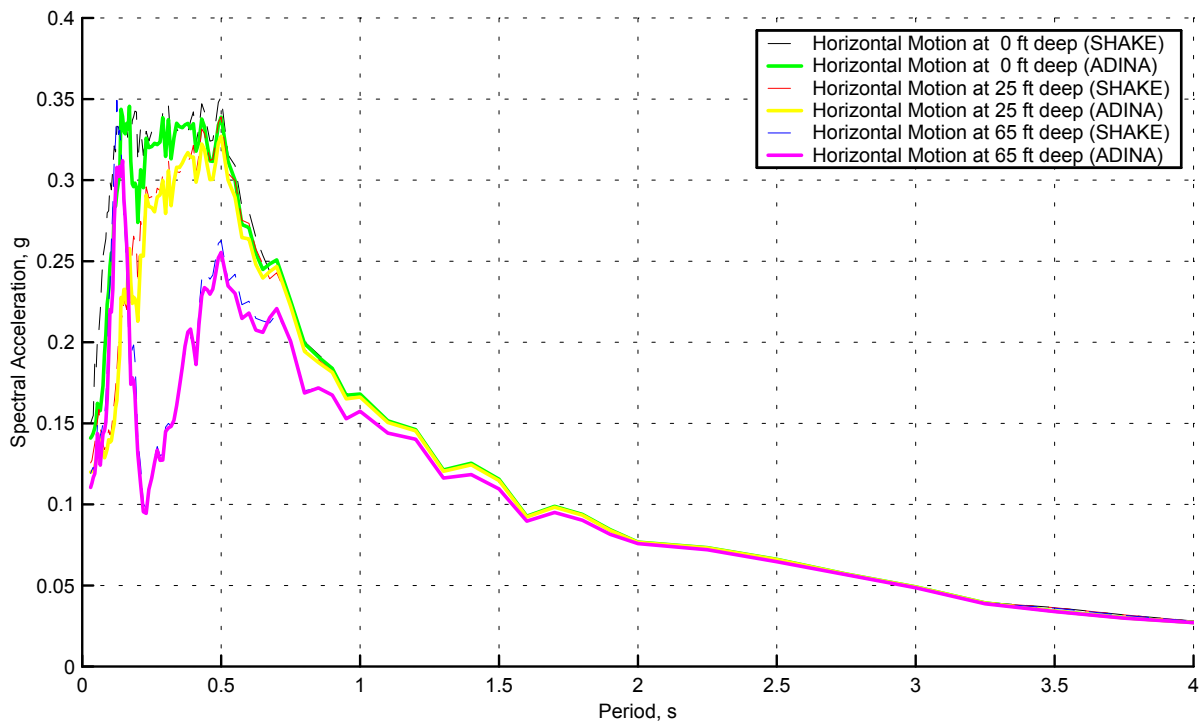


Figure II-16. Two Component Motions for ADINA Model with Slaving Left and Right Boundaries

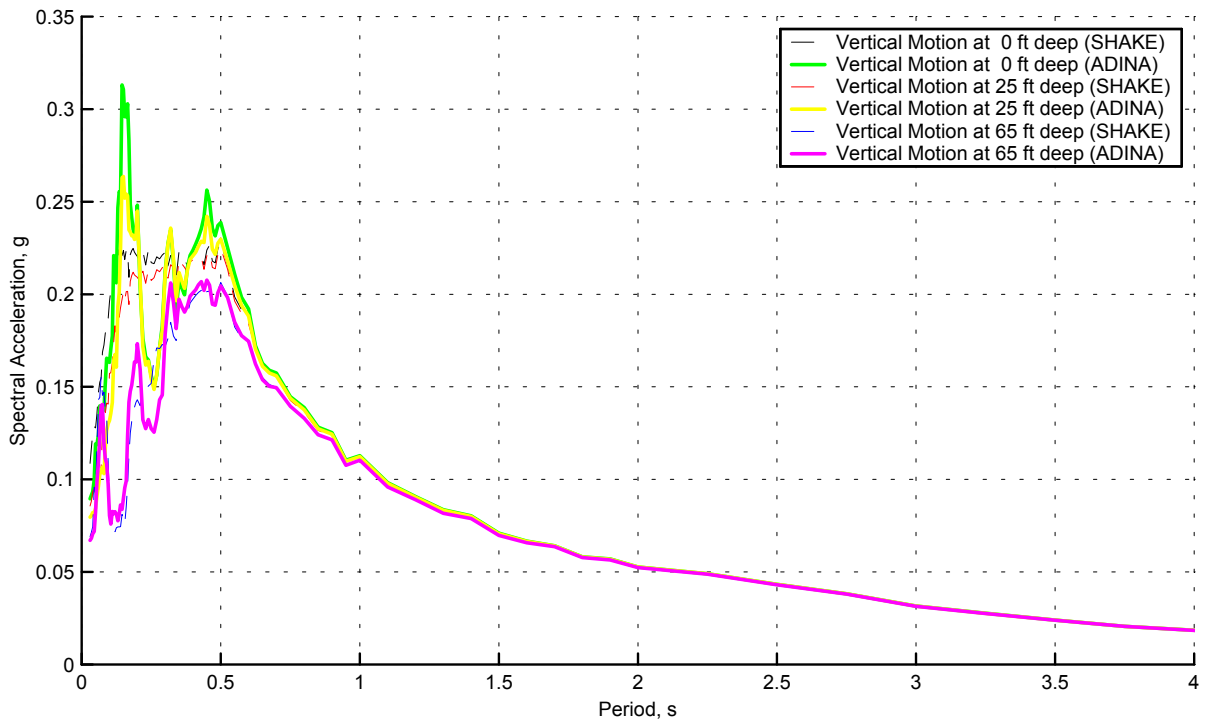
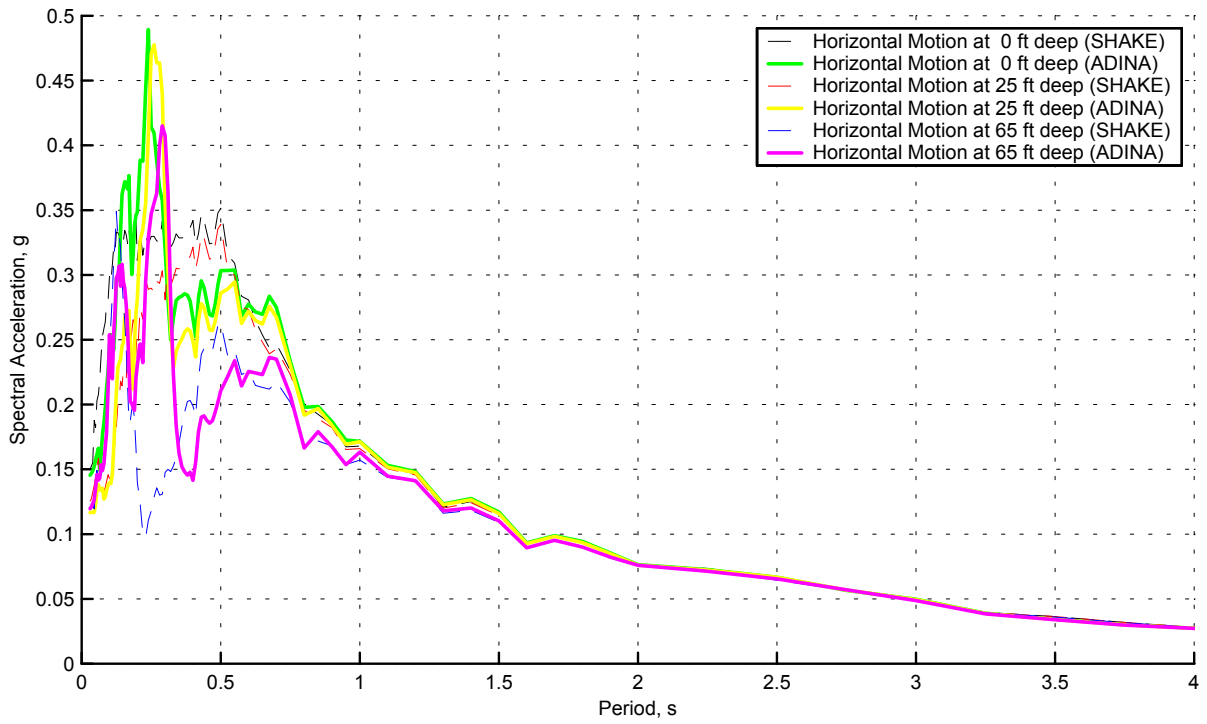


Figure II-17. Two Component Motions for ADINA Model with Two Edge Columns

Deformations are amplified 1000 times (Vertical Motion Only)

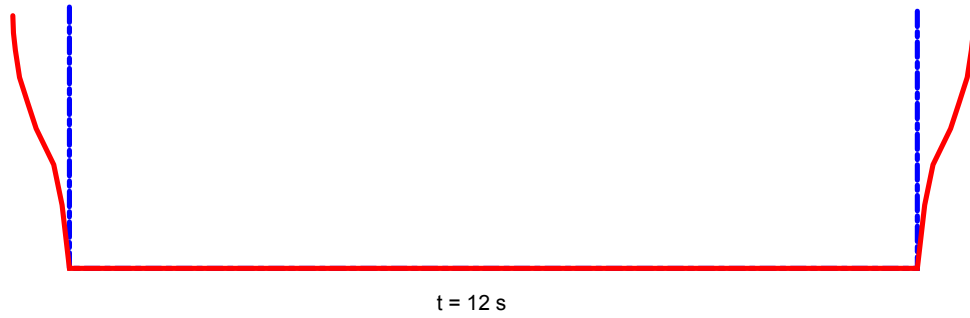
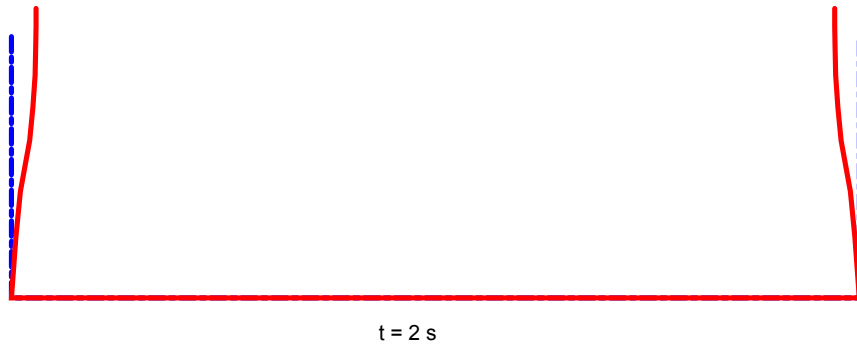


Figure II-18. Snapshots of Profile of Side Boundary